Transfer of III-nitride epitaxial layers onto pre-patterned silicon substrates for the simple fabrication of free-standing MEMS

Rajat Gujrati, Ali Kassem, Cédric Ayela, Fabrice Mathieu, Liviu Nicu, Suresh Sundaram, Isabelle Dufour, William Hunt, Abdallah Ougazzaden, Jean-Paul Salvestrini, et al.

Transfer of III-Nitride epitaxial layers onto pre-patterned silicon substrates for the simple fabrication of free-standing MEMS

Rajat Gujrati[1], Ali Kassem[1], Cédric Ayela[2], Fabrice Mathieu[3], Liviu Nicu[3], Suresh Sundaram[1,4], Isabelle Dufour[2], William Hunt[5], Abdallah Ougazzaden[1,5], Jean-Paul Salvestrini[1,4,5], and Thierry Leichlé[1,3,5,*]

[1]CNRS, IRL 2958 Georgia Tech-CNRS, Metz, France

[2]Université de Bordeaux, Laboratoire IMS UMR-CNRS 5218, Talence, France

[3]LAAS-CNRS, Toulouse, France

[4]Georgia Tech Europe, IRL 2958 Georgia Tech-CNRS, Metz, France

[5]Georgia Institute of Technology, School of Electrical and Computer Engineering, IRL 2958 Georgia Tech-CNRS, Atlanta, GA, USA

[*]Corresponding author: thierry.leichle@cnrs.fr

Abstract

In recent years, the remarkable properties and potential applications of III-nitride (III-N) semiconductors have sparked a significant interest in the field of microelectromechanical systems (MEMS). Traditionally III-N MEMS are fabricated through a process involving the epitaxial growth of III-N epilayers on a silicon substrate followed by etching the handle wafer to generate free-standing structures. In this study, we explore the potential of a relatively simple approach based on the two-dimensional (2D) material-based lift-off and transfer, to fabricate III-N mechanical resonators. The methodology involves van der Waals epitaxy of III-N layers on 2D hexagonal-boron nitride (h-BN), which leverage weak van der Waals adhesion between h-BN layers, to lift-off and transfer these layers from their original growth substrate to an alternative host substrate. The employed method is demonstrated by fabricating 600 nm thick GaN/AlGaN and 2.5 µm thick h-BN micro-resonators onto pre-patterned cavities etched in silicon substrates. These devices are characterized using laser Doppler vibrometry, enabling the observation of well-defined modes of vibration and resonant frequencies. Further, finite element method simulations are performed to gain insights into the experimental observations and the mechanical properties of the transferred layers. This approach could be extended to transfer high-quality III-N MEMS devices onto various host substrates, including flexible substrates, and could be used to assess the mechanical properties of emerging III-N semiconductor materials.

Gallium Nitride (GaN) has garnered a significant attention in the field of microelectromechanical systems (MEMS) due to its intrinsic crystalline quality stemming from its wurtzite crystal structure,[1] notable wide bandgap,[2] piezoelectric and piezoresistive characteristics,[1,3,4] high temperature stability,[5,6] chemical robustness,[7] and seamless integration capabilities with GaN electronics.[8,9] Moreover, the AlGaN/GaN interface hosts a two-dimensional electron gas (2-DEG)[10,11] that can function as a strain transducer with enhanced sensitivity due to its exceptional sheet carrier concentration (>10^{13} cm^{-2}) and electron mobility (>2000 cm^2/Vs), without intentional doping.[1,12,13] These outstanding attributes of AlGaN/GaN heterostructures position them as highly promising candidates for MEMS operations demanding high-frequency capabilities, superior performance and sensitivity.[13–15]

GaN MEMS innovative components and systems include GaN Lamb wave resonators,[16] GaN-on-SOI resonators catering to infrared detection,[17] and GaN-on-silicon filters designed for specific filtration purposes.[18] The conventional process for fabricating GaN MEMS involves growing GaN epitaxial layers on silicon substrates, followed by substrate etching to create free-standing structures.[1,13–15] Silicon substrates are advantageous for easy micromachining but pose challenges for achieving high-quality crystalline III-N layers.[1,19] GaN-on-silicon substrates commonly exhibit high threading dislocation densities, mainly screw-type dislocations.[20]

The heterogeneous integration of GaN MEMS to substrates that are not well-suited for epitaxy (*e.g.,* flexible substrates) typically requires thin film transfer method, which involves isolating grown epilayers from their initial growth substrate for subsequent transfer onto the desired host substrate. Methods like laser lift-off,[21,22] ion implantation-induced interface splitting,[23,24] and wet etching[25,26] serve this purpose. However, these approaches have limitations including slow processing, laser-induced interface damage, material constraints, limited thickness options, and potential ionic contamination.[26–28] Alternatively, the 2D material-based layer transfer (2DLT) technique is also pioneered[29,30] that uses h-BN as a sacrificial layer for the lift-off and transfer of III-N layers grown on h-BN/sapphire templates to foreign substrates. Owing to the weak van der Waals interactions within the h-BN layers, the III-N epilayers can be mechanically lifted-off from their native sapphire substrate, providing a route for convenient transfer onto another substrate. The adoption of this approach offers the potential for recycling the growth sapphire substrate, leading to reduced footprint and cost effectiveness. Notably this technique has been used to fabricate flexible HEMTs gas sensors,[31] LEDs,[32–34] and solar cells.[35]

In this context, this paper extends the 2DLT technique to the fabrication of free-standing III-N MEMS. This approach eliminates the requirement for etching a substrate or a sacrificial layer to release the movable parts of the microsystem; instead, the III-N layers are transferred to pre-patterned substrates. In order to validate the viability of the proposed technique, this study focuses on the process of lifting-off and transferring epitaxial layers of GaN (300 nm)/AlGaN (300 nm), grown onto a 3 nm h-BN sacrificial layer/sapphire template, onto pre-patterned cavities etched in silicon substrates. Furthermore, this study underscores that h-BN can serve as more than just a transfer sacrificial layer; it also possesses the potential to function as the active layer in MEMS. This is accomplished by transferring 2.5 µm thick h-BN epilayers grown on sapphire onto pre-patterned silicon substrates. The AlGaN/GaN bi-layer and h-BN thin films are suspended above 180 µm × 60 µm and 450 µm × 150 µm rectangular cavities, respectively. Dynamic characterizations were performed on both structures. Finite element method (FEM) simulations using COMSOL were conducted to obtain the eigenfrequencies and the shapes of the first resonant modes and to gain insights into the experimental observations. In summary, this study demonstrates the transfer and the integration of III-N epitaxial layers onto pre-patterned silicon substrates. The method can be extended to different substrates, rigid or flexible, thereby enhancing the versatility of device integration and advancing the field of III-N MEMS fabrication.

The schematic representation of the pick and place process employed for the fabrication of self-standing III-N MEMS resonators is depicted in Figure 1. The process starts with the lift-off of the III-N epilayers grown on the h-BN/sapphire template, by employing a 15 mm × 15 mm double-side water tape affixed to a stamp. The stamp is gently lowered to stick to the epilayer on the sapphire substrate (Fig. 1(a)). During the pick-up step, pressure is first applied on the stamp during 30 s to ensure the uniform adhesion of the adhesive tape to the epilayer, followed by the swift raise of the stamp at a speed of 1 mm/s (Fig. 1(b)). Then the III-N layer is transferred onto a host substrate using capillary assembly where the drying of a water film at the interface of the III-N film and the substrate is used to create large surface area to promote adhesion via van der Waals forces.[33] To this aim, after lifting the III-N layers with the stamp, a thin film of water is applied using a wetted microscope lens wipes (Fig. 1(c)). The stamp is then positioned atop of a silicon substrate patterned with micro-cavities (Fig. 1(d)). The placement process first entails lowering the stamp until the III-N thin film contacts the silicon surface. Then, a pressing force of 50 mN (equivalent to stamp weight of ~5 grams) is exerted for 1 min to facilitate the wetted III-N film's adhesion to the silicon substrate through capillary forces. Following placement, the stamp is removed, by dissolving the water tape upon immersion of the silicon sample along with the stamp in a water-filled beaker for 30 min (Fig. 1(e)). This final step removes the stamp, leaving the III-N epilayer, held by van der Waals forces, on the silicon sample. The presence of the cavities in the silicon substrate results in the formation of self-standing structures.

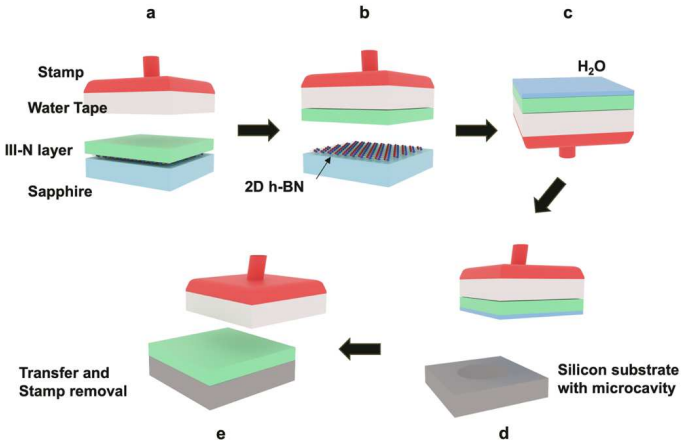

FIG. 1. Schematics of the proposed method for the fabrication of free standing III-N MEMS on a host substrate by a lift-off and transfer process (where the III-N layer is GaN/AlGaN or BN). (a), (b) Water tape is used to pick up the epilayer grown onto h-BN/sapphire template. (c), (d) The epilayer is transferred using pressure and capillary forces onto a silicon substrate with etched cavities and (e) the stamp is dissolved to obtain the self-standing III-N structure held to the silicon substrate by van der Waals forces.

Two sets of samples are used in this study: (1) a GaN (300 nm)/$Al_{0.14}Ga_{0.86}N$ (300 nm) heterostructure grown onto a 3 nm h-BN/sapphire template and (2) a 2.5 µm-thick h-BN epilayer grown on a sapphire substrate. These samples are grown on epi-ready sapphire substrates in a closed coupled showerhead (CCS 3×2'') reactor by metal-organic chemical vapor deposition (MOCVD) technique. The growth conditions are described in great detail in previous works.[31,36] Figure 2 shows the high-resolution X-ray diffraction (HR-XRD) 2θ-ω scans of the GaN/AlGaN heterostructure (Fig. 2(a)), and the 2.5 µm h-BN film grown on sapphire (Fig. 2(b)). As evident in the figure, diffraction peaks for the GaN/AlGaN heterostructure are observed at 34.5° and 34.7°, corresponding to the (002) reflections of GaN and AlGaN layers, respectively. The HR-XRD 2θ-ω scan for the h-BN layer exhibits a discernible peak at 25.8°, which corresponds to the (0002) planes of the sp^2 BN. It is worth noting the presence of an AlN peak at 36.3° in the scan, which is attributed to the nitridation of the sapphire substrate during growth (utilizing NH_3 flow) that preceded the h-BN growth.

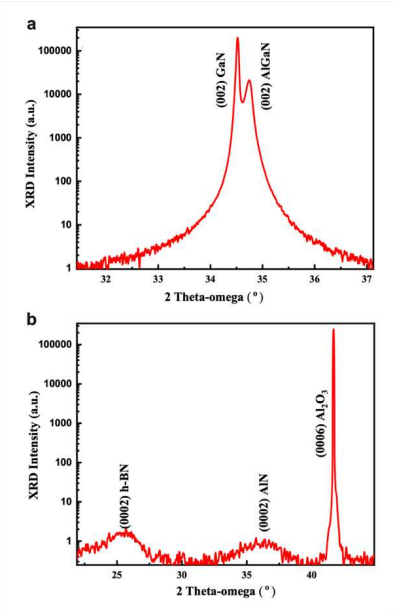

FIG. 2. High-resolution X-ray diffraction (HR-XRD) 2θ – ω scans (a) of the 300 nm GaN/300 nm AlGaN heterostructure on 3 nm h-BN/sapphire wafer, and (b) of the 2.5 μm thick h-BN epilayer on sapphire wafer.

The host silicon substrate with pre-patterned cavities is obtained by etching cavities of various geometries and sizes by deep reactive ion etching (DRIE). Standard 100 mm, P-type silicon wafers are used for this purpose and the patterns are created using AZ 125NXT photoresist and an Alcatel AMS 4200 for dry etching of silicon. Among others, cavities of 180 μm × 60 μm and 450 μm × 150 μm rectangular shapes and 22 μm deep are obtained. After the etching process, the photoresist is removed using AZ100 remover followed by an oxygen plasma treatment (Tepla). The wafers are then cleaved into chips, of size ~ 4 cm × 1.5 cm, onto which transfer of III-N layers is performed.

Figure 3 provides a summary of the transfer results of the GaN (300 nm)/AlGaN (300 nm) layers onto silicon substrates with microcavities. Optical and scanning electron microscopy (SEM) observations were employed to examine the transferred layer, revealing anticipated transparent and opaque surface under optical and SE microscopy, respectively (Fig. 3(a)). Notably, the transparency of the layer under the optical microscope facilitates the visualization of the cavity's interior and bottom through the thin film overlay (Fig. 3(b)). Importantly, Figure 3(b) showcases a cavity free from any contaminants. This ensures that the intended function of the cavity, namely to provide free space for structural deformation of the transferred film, remains unchanged after the film transfer process. Additionally, SEM observations (Fig. 3(c)) of the transferred epilayers on the cavities show the absence of GaN morphology degradation following the transfer procedure.

The transfer process of the 2.5 μm thick h-BN layer, which is identical to the process used to transfer GaN/AlGaN layers, was carried out on silicon microcavities and results are shown in Figure 4. The structures were further observed with an optical profilometer (Veeco NT9080), and the resulting images (Fig. 4(c)) indicate that the h-BN layer covering the cavity is flat and adhere uniformly to the silicon surface with clean edge clamping (the step observed at the edge of the cavities is an interface artifact of the profilometer).

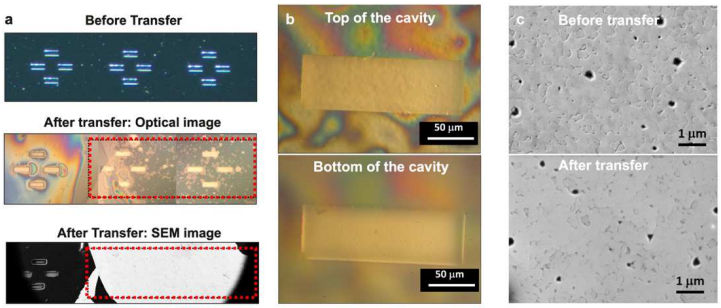

FIG. 3. (a) Silicon substrate with microcavities before and after transferring a GaN/AlGaN layer observed by optical microscopy and SEM (the location of the transferred film is indicated by the red dashed rectangle), (b) Inside of a cavity covered by a GaN/AlGaN film observed by optical microscopy, (c) Surface morphology of the GaN surface before and after transfer observed by SEM.

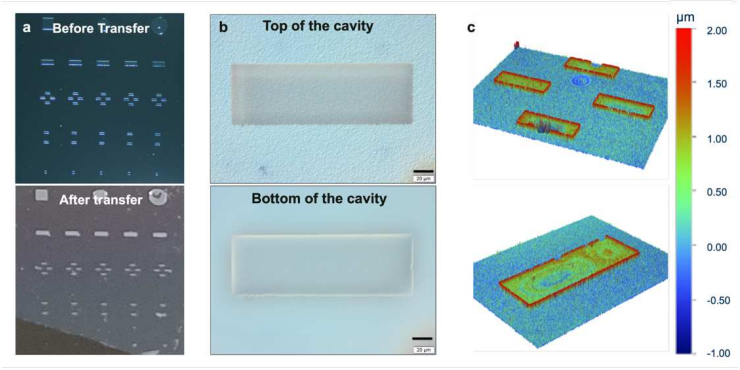

FIG. 4. (a) Optical images of the cavities before and after transfer of 2.5 µm thick h-BN. (b) Observation of the cavity interior with optical microscopy by focusing on the top and bottom of the cavity (scale bar 20 µm). (c) Optical profilometer images of the h-BN plates covering the cavities etched in the silicon wafer.

Next, the mechanical characterization of the fabricated free-standing GaN/AlGaN and h-BN plates was conducted by performing dynamic studies of the corresponding mechanical resonators. To this aim, the silicon samples were mounted on a PZT piezoelectric actuator used as an external mechanical excitation source. The displacement of the self-standing layers was mapped using a laser Doppler vibrometer (MSA-500 Micro System Analyzer from Polytec) upon actuation. The amplitude of vibration of the resonator was recorded while sweeping the excitation frequency.

Figure 5 shows the dynamic response of a 300 nm GaN/300 nm AlGaN heterostructure transferred onto a 22 µm deep, 180 µm × 60 µm rectangular silicon cavity. The resonant frequency peaks of the first three consecutive flexural modes of resonance are displayed in Figure 5(a). Peaks were clearly identified from the corresponding mode shapes (Fig. 5(b)), resulting in measured resonance frequencies of 1.39 MHz, 1.58 MHz and 1.85 MHz. Analogously, the first resonance modes of 450 µm × 150 µm rectangular 2.5 µm thick h-BN plates were characterized. Figure 6(a) shows the shapes of the first and the third observed modes with the corresponding displacement profiles at resonance along the length of the plate through its center (Fig. 6(b)).

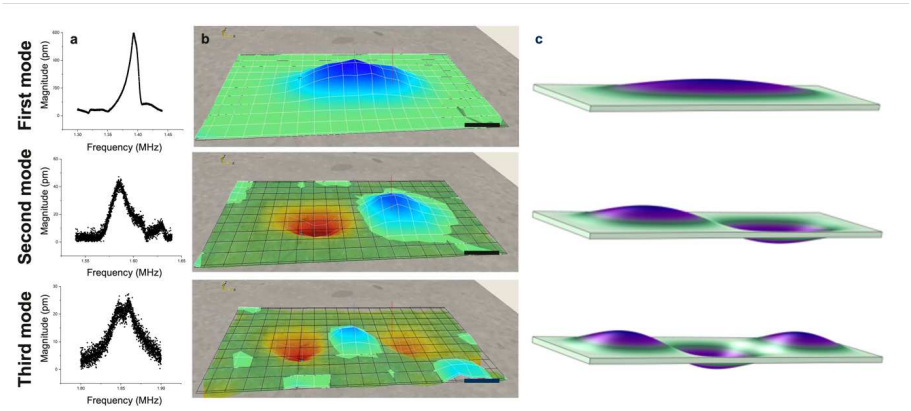

FIG. 5. (a) Resonance spectra of the first three modes of a rectangular AlGaN/GaN plate on silicon (where the amplitude of vibration is measured at the largest displacement location, which depends on the mode shape); (b) corresponding measured 3D displacement maps showing the maximum deflection amplitude of first three modes (scale bars: 20μm); (c) COMSOL simulation of the three modes of vibration.

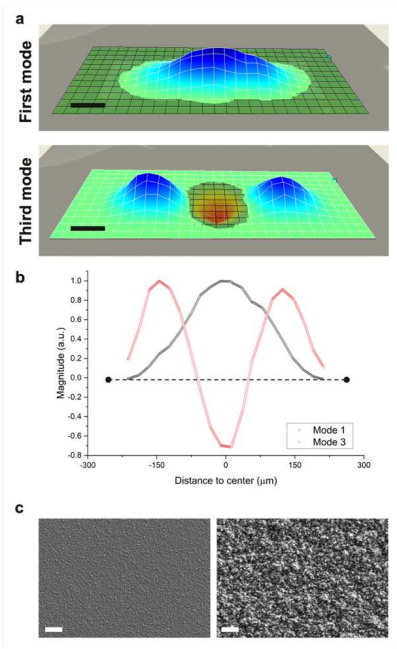

FIG. 6. (a) Measured resonance modes of the h-BN micro-resonator (scale bars: 50μm); (b) normalized deflection profile of the film at the line of maximum deflection; and (c) SEM image of the 2.5 μm thick h-BN epilayer grown on a sapphire wafer (scale bar: left= 10 μm, right= 1 μm).

The natural frequencies of the mode of a rectangular plate is given by:[37]

$$f_{ij} = \frac{\lambda_{ij}^2}{2\pi a^2}\left[\frac{Eh^3}{12\gamma(1-\nu^2)}\right]^{1/2}$$

where *a* and *h* are the plate length and thickness, respectively, *i* and *j* are the number of half-waves in mode shape along the length and width, *E* is the modulus of elasticity of the plate, ν is the Poisson's ratio and γ is the mass per unit area. λ is a dimensionless frequency parameter that depends on the clamping conditions (boundary conditions applied at the edges of the plate), the plate length to width ratio and the mode number. The mode sequence and the frequency ratio between a given mode and the fundamental mode are an indication of the boundary conditions (free, clamped, supported): in our case, we experimentally observed that the first three modes are the (11), (21), (31) modes with measured frequency and frequency ratio listed in Table 1.

FEM simulations were performed using COMSOL to determine the eigenfrequencies and mode shapes of a bi-layer AlGaN/GaN thin film and a h-BN film suspended on a 180 µm × 60 µm and a 450 µm × 150 µm rectangular cavity, respectively. Values for the Poisson's ratio and the density for all plate materials were those found in the literature (with ν_{AlGaN} =0.2,[38] ν_{GaN} =0.18,[39] ν_{BN} =0.21,[40] ρ_{AlGaN} =5304 kg/m^3,[41] ρ_{GaN} =6150 kg/m^3,[1,41] ρ_{BN} =2100 kg/m^3)[42], and the Young's modulus was used as an adjusting parameter. Simulations were conducted with fully clamped boundary conditions at the edge of the cavity according to the measured mode sequence and the frequency ratios.[37]

Figure 5(c) shows the first three simulated modes of the AlGaN/GaN resonator that are in the same sequential order of the observed experimental modes. Table 1 summarizes the theoretical and experimental resonance frequencies of the first three modes along with the calculated frequency ratios of the n-mode over the fundamental mode (*i.e.,* $\lambda_{ij}^2/\lambda_{11}^2$). It is important to note that using the typical Young's modulus values found in the literature (*i.e.,* E_{GaN} =261 GPa and E_{AlGaN} =285 GPa)[41] results in theoretical values of the resonance frequencies and frequency ratios close to the experimental ones.

The sequence of the modes obtained by simulation is also the same as the experimental ones for the h-BN plate. However, the Young's modulus value that leads to theoretical results (in terms of resonance frequency and frequency ratios) in agreement with experimental values is E_{BN} =18 GPa, which is far from the ≈0.8 TPa value consistently reported in the literature for single layer h-BN.[40] This later value, which is fairly constant for up to 8 h-BN sheets, has been estimated to be much lower for thicker layers. For instance, the Young's modulus of 292 nm thick pristine h-BN flakes exfoliated from their layered bulk was estimated at 248 GPa.[43] Also the modulus of ≈100-120 nm thin films BN synthetized by pulsed laser deposition was measured in the range of 120-180 GPa using nanoindentation.[44] But these values are still far from the one derived from our parametrical fit. Hence, we have used FEM to take into account other parameters that could account for this large discrepancy in modulus, namely the presence of internal stress (since the h-BN layer is lifted from the substrate, it should be stress-free, however additional stress could be induced during the transfer process) or modified clamping conditions that would influence the size of the plate. Simulations were conducted with E_{BN} =120 GPa, the lowest value found in the literature,[44] and either the internal stress or the plate size was adjusted to fit the resonant frequency of the first mode to the experimental value. Table 1 presents the corresponding results. A fit is obtained for a bi-axial compressive stress of ≈-95 MPa, which seems large when compared to the stress of, for instance, silicon dioxide thermally grown onto silicon that is generally of the order of a few hundred MPa.[45] Besides and more importantly, the resonance frequencies of higher modes do not match. On the other hand, a good correspondence between simulated and experimental frequencies is obtained for E_{BN} =120 GPa and a plate size of 725 µm × 241 µm, which is 1.6^2 time larger than the actual plate size. However, the profiles of the plate for the first and the third modes at maximum amplitude deflection (Fig. 6(b)) tend to indicate that the length of the plate corresponds to the size of the cavity. Hence, these hypotheses are not fully satisfactory, and we stipulate that the Young's modulus of our grown h-BN layer must be lower than what was previously reported. The presence of AlN (as illustrated from Fig. 2) in between the sapphire substrate and the BN layer should not influence the mechanical properties of the plate since it is very unlikely that the AlN would delaminate during the lift because it forms a 3D epitaxial bonds with sapphire (which is much stronger than the inter h-BN layer van der Waals interactions). In fact, a low Young's modulus could be explained from the growth process leading to distinct structural

properties of our BN. Indeed, SEM observations of the h-BN surface (Fig. 6(c)) indicate a granular surface morphology, which is owed to the high growth rate (470 nm/h), causing transition from layered to turbo static growth mode of h-BN layers.[36] As a result, following the two-dimensional h-BN structure formed at the film/sapphire interface, the top h-BN layer is organized in short domains irregularly oriented, losing long range order, which could explain our observations.

Table 1. Experimental and simulated values of measured resonant frequencies.

	$Al_{0.14}Ga_{0.86}N$/GaN Plate				BN Plate							
Thickness	300 nm / 300 nm				2500 nm							
Dimensions	180 µm × 60 µm				450 µm × 150 µm							
Resonance modes	Experiment		FEM E_{GaN}= 261 GPa E_{AlGaN}= 285 GPa		Experiment		FEM E_{hBN}= 18 GPa		FEM E_{hBN}= 120 GPa x×y= 725 × 241 µm²		FEM E_{hBN}= 120 GPa σ_{11}= σ_{22}= -95.5 MPa	
	Frequency (kHz)	Ratio	Frequency (kHz)	Ratio	Frequency (kHz)	Ratio	Frequency (kHz)	Ratio	Frequency (kHz)	Ratio	Frequency (kHz)	Ratio
Mode 1	1390	-	1248	-	355	-	354	-	355	-	355	-
Mode 2	1580	1.14	1391	1.11	-	-	394	1.11	395	1.11	382	1.07
Mode 3	1850	1.33	1654	1.32	476	1.34	469	1.32	469	1.32	531	1.49
Mode 4	-	-	-	-	604	1.7	581	1.64	580	1.63	814	2.30
Mode 5	-	-	-	-	782/812	2.20/2.28	731	2.06	730	2.05	1209	3.40

The passive resonators fabricated by the pick-and-place method introduced in this work have been shown to vibrate with well-defined modes of vibration and resonant frequencies in agreement with theoretical studies conducted using the FEM, at least in the case of AlGaN/GaN epilayers-based plate resonators. This simple method can be used in the determination of the mechanical properties of III-N layers, such as the h-BN thick film used in this study. Moreover, the fabrication of active MEMS integrating transduction schemes can be envisioned by carefully controlling and optimizing each fabrication step after growth to avoid spontaneous delamination of the device that could arise from mechanical strains, as it has been demonstrated with the fabrication of HEMT devices on 2D h-BN.[31] Most importantly, the adopted approach of pick-and-place of epilayers and their transfer to pre-patterned cavities can also be extended to the fabrication of flexible GaN MEMS. Indeed, although we have tested the viability of this method on a silicon substrate, we foresee that it can be extended to flexible substrates, such as polyethylene terephthalate (PET) or Kapton. The realization of flexible III-N MEMS, that are difficult to manufacture through conventional micromachining processes, would open the door to a wide range of applications, from wearable devices for health monitoring to the internet of things, even if further technical developments are needed to reach the level of yield and device performance offered by conventional fabrication methods.

ACKOWLEDGMENTS

This work was supported by the French National Research Agency (ANR) under the research project FLEXIGAN (grant ANR-22-CE51-0009), by FLEXMEMS (IC ARTS), and partially by INMOST (grant ANR-19-CE08-0025), by the Region Grand Est in France and by the French national technological network RENATECH. The authors acknowledge contributions from Dr. Soufiane Karrakchou and Adama M'Ballo during the initial phase of the project. The authors also thank Mr. Vishnu Ottapilakkal, for his help in performing the XRD measurements.

AUTHOR DECLARATIONS

Conflict of Interest

The authors have no conflicts to disclose.

Author Contributions

Rajat Gujrati: Investigation (equal); Visualization (equal); Writing/Original Draft Preparation (equal). Ali Kassem: Investigation (equal); Writing/Original Draft Preparation (equal). Cédric Ayela: Investigation (equal). Fabrice Mathieu: Investigation (equal). Liviu Nicu: Investigation (equal); Writing/Review & Editing (equal). Suresh Sundaram: Investigation (equal). Isabelle Dufour: Writing/Review & Editing (equal). William Hunt: Writing/Review & Editing (equal). Abdallah Ougazzaden: Funding Acquisition (supporting), Resources (equal). Jean-Paul Salvestrini: Conceptualization (equal); Funding Acquisition (equal); Resources (equal); Writing/Review & Editing (equal). Thierry Leichlé: Conceptualization (lead); Funding Acquisition (lead); Investigation (equal); Visualization (equal); Writing/Original Draft Preparation (equal); Writing/Review & Editing (equal).

DATA AVAILABILITY

The data that support the findings of this study are available from the corresponding author upon reasonable request.

REFERENCES

[1] M. Rais-Zadeh, V.J. Gokhale, A. Ansari, M. Faucher, D. Theron, Y. Cordier, and L. Buchaillot, "Gallium Nitride as an Electromechanical Material," J. Microelectromech. Syst. **23**(6), 1252–1271 (2014).
[2] J. Kolník, İ.H. Oğuzman, K.F. Brennan, R. Wang, P.P. Ruden, and Y. Wang, "Electronic transport studies of bulk zincblende and wurtzite phases of GaN based on an ensemble Monte Carlo calculation including a full zone band structure," Journal of Applied Physics **78**(2), 1033–1038 (1995).
[3] A.D. Bykhovski, V.V. Kaminski, M.S. Shur, Q.C. Chen, and M.A. Khan, "Piezoresistive effect in wurtzite *n* -type GaN," Applied Physics Letters **68**(6), 818–819 (1996).
[4] R. Gaska, J.W. Yang, A.D. Bykhovski, M.S. Shur, V.V. Kaminskii, and S. Soloviov, "Piezoresistive effect in GaN–AlN–GaN structures," Applied Physics Letters **71**(26), 3817–3819 (1997).
[5] H. Ishikawa, K. Yamamoto, T. Egawa, T. Soga, T. Jimbo, and M. Umeno, "Thermal stability of GaN on (1 1 1) Si substrate," Journal of Crystal Growth **189–190**, 178–182 (1998).
[6] I. Daumiller, C. Kirchner, M. Kamp, K.J. Ebeling, and E. Kohn, "Evaluation of the temperature stability of AlGaN/GaN heterostructure FETs," IEEE Electron Device Lett. **20**(9), 448–450 (1999).
[7] D.-H. Lien, Y.-H. Hsiao, S.-G. Yang, M.-L. Tsai, T.-C. Wei, S.-C. Lee, and J.-H. He, "Harsh photovoltaics using InGaN/GaN multiple quantum well schemes," Nano Energy **11**, 104–109 (2015).
[8] Amano, H.; Baines, Y.; Beam, E.; Borga, M.; The 2018 GaN Power Electronics Roadmap. *J. Phys. D: Appl. Phys.* **2018**, *51* (16), 163001. https://doi.org/10.1088/1361-6463/aaaf9d.
[9] S.J. Pearton, and F. Ren, "GaN Electronics," Adv. Mater. **12**(21), 1571–1580 (2000).
[10] S. Khandelwal, N. Goyal, and T.A. Fjeldly, "A Physics-Based Analytical Model for 2DEG Charge Density in AlGaN/GaN HEMT Devices," IEEE Trans. Electron Devices **58**(10), 3622–3625 (2011).
[11] K. Abgaryan, I. Mutigullin, and D. Reviznikov, "Theoretical investigation of 2DEG concentration and mobility in the AlGaN/GaN heterostructures with various Al concentrations," Phys. Status Solidi C **12**(12), 1376–1382 (2015).
[12] K. Brueckner, F. Niebelschuetz, K. Tonisch, S. Michael, A. Dadgar, A. Krost, V. Cimalla, O. Ambacher, R. Stephan, and M.A. Hein, "Two-dimensional electron gas based actuation of piezoelectric AlGaN/GaN microelectromechanical resonators," Applied Physics Letters **93**(17), 173504 (2008).
[13] L.C. Popa, and D. Weinstein, in *2013 Joint European Frequency and Time Forum & International Frequency Control Symposium (EFTF/IFC)* (IEEE, Prague, Czech Republic, 2013), pp. 922–925.
[14] L.C. Popa, and D. Weinstein, in *2013 Transducers & Eurosensors XXVII: The 17th International Conference on Solid-State Sensors, Actuators and Microsystems (TRANSDUCERS & EUROSENSORS XXVII)* (IEEE, Barcelona, Spain, 2013), pp. 2461–2464.
[15] J. Dzuba, G. Vanko, M. Držík, I. Rýger, V. Kutiš, J. Zehetner, and T. Lalinský, "AlGaN/GaN diaphragm-based pressure sensor with direct high performance piezoelectric transduction mechanism," Applied Physics Letters **107**(12), 122102 (2015).

[16] H. Zhu, A. Ansari, and M. Rais-Zadeh, in *2016 Compound Semiconductor Week (CSW) [Includes 28th International Conference on Indium Phosphide & Related Materials (IPRM) & 43rd International Symposium on Compound Semiconductors (ISCS)* (IEEE, Toyama, Japan, 2016), pp. 1–2.
[17] V.J. Gokhale, and M. Rais-Zadeh, "Uncooled Infrared Detectors Using Gallium Nitride on Silicon Micromechanical Resonators," J. Microelectromech. Syst. **23**(4), 803–810 (2014).
[18] A. Ansari, V.J. Gokhale, V.A. Thakar, J. Roberts, and M. Rais-Zadeh, in *2011 International Electron Devices Meeting* (IEEE, Washington, DC, USA, 2011), p. 20.3.1-20.3.4.
[19] L. Liu, and J.H. Edgar, "Substrates for gallium nitride epitaxy," Materials Science and Engineering: R: Reports **37**(3), 61–127 (2002).
[20] Y. Cordier, N. Baron, S. Chenot, P. Vennéguès, O. Tottereau, M. Leroux, F. Semond, and J. Massies, "Strain engineering in GaN layers grown on silicon by molecular beam epitaxy: The critical role of growth temperature," Journal of Crystal Growth **311**(7), 2002–2005 (2009).
[21] Jaeyi Chun, Youngkyu Hwang, Yong-Seok Choi, Tak Jeong, Jong Hyeob Baek, Heung Cho Ko, and Seong-Ju Park, "Transfer of GaN LEDs From Sapphire to Flexible Substrates by Laser Lift-Off and Contact Printing," IEEE Photon. Technol. Lett. **24**(23), 2115–2118 (2012).
[22] T. Ueda, M. Ishida, and M. Yuri, "Separation of Thin GaN from Sapphire by Laser Lift-Off Technique," Jpn. J. Appl. Phys. **50**(4R), 041001 (2011).
[23] R. Singh, S.H. Christiansen, O. Moutanabbir, and U. Gösele, "The Phenomenology of Ion Implantation-Induced Blistering and Thin-Layer Splitting in Compound Semiconductors," Journal of Elec Materi **39**(10), 2177–2189 (2010).
[24] O. Moutanabbir, R. Scholz, S. Senz, U. Gösele, M. Chicoine, F. Schiettekatte, F. Süßkraut, and R. Krause-Rehberg, "Microstructural evolution in H ion induced splitting of freestanding GaN," Applied Physics Letters **93**(3), 031916 (2008).
[25] D. Simeonov, E. Feltin, A. Altoukhov, A. Castiglia, J.-F. Carlin, R. Butté, and N. Grandjean, "High quality nitride based microdisks obtained via selective wet etching of AlInN sacrificial layers," Applied Physics Letters **92**(17), 171102 (2008).
[26] D. Zhuang, and J.H. Edgar, "Wet etching of GaN, AlN, and SiC: a review," Materials Science and Engineering: R: Reports **48**(1), 1–46 (2005).
[27] C.R. Giuliano, "Laser-induced damage in transparent dielectrics: ion beam polishing as a means of increasing surface damage thresholds," Applied Physics Letters **21**(1), 39–41 (1972).
[28] K. Hjort, "Sacrificial etching of III - V compounds for micromechanical devices," J. Micromech. Microeng. **6**(4), 370–375 (1996).
[29] Y. Kobayashi, K. Kumakura, T. Akasaka, and T. Makimoto, "Layered boron nitride as a release layer for mechanical transfer of GaN-based devices," Nature **484**(7393), 223–227 (2012).
[30] J. Kim, C. Bayram, H. Park, C.-W. Cheng, C. Dimitrakopoulos, J.A. Ott, K.B. Reuter, S.W. Bedell, and D.K. Sadana, "Principle of direct van der Waals epitaxy of single-crystalline films on epitaxial graphene," Nat Commun **5**(1), 4836 (2014).
[31] T. Ayari, C. Bishop, M.B. Jordan, S. Sundaram, X. Li, S. Alam, Y. ElGmili, G. Patriarche, P.L. Voss, J.P. Salvestrini, and A. Ougazzaden, "Gas sensors boosted by two-dimensional h-BN enabled transfer on thin substrate foils: towards wearable and portable applications," Sci Rep **7**(1), 15212 (2017).
[32] J. Shin, H. Kim, S. Sundaram, J. Jeong, B.-I. Park, C.S. Chang, J. Choi, T. Kim, M. Saravanapavanantham, K. Lu, S. Kim, J.M. Suh, K.S. Kim, M.-K. Song, Y. Liu, K. Qiao, J.H. Kim, Y. Kim, J.-H. Kang, J. Kim, D. Lee, J. Lee, J.S. Kim, H.E. Lee, H. Yeon, H.S. Kum, S.-H. Bae, V. Bulovic, K.J. Yu, K. Lee, K. Chung, Y.J. Hong, A. Ougazzaden, and J. Kim, "Vertical full-colour micro-LEDs via 2D materials-based layer transfer," Nature **614**(7946), 81–87 (2023).
[33] S. Karrakchou, S. Sundaram, T. Ayari, A. Mballo, P. Vuong, A. Srivastava, R. Gujrati, A. Ahaitouf, G. Patriarche, T. Leichlé, S. Gautier, T. Moudakir, P.L. Voss, J.P. Salvestrini, and A. Ougazzaden, "Effectiveness of selective area growth using van der Waals h-BN layer for crack-free transfer of large-size III-N devices onto arbitrary substrates," Sci Rep **10**(1), 21709 (2020).
[34] R. Gujrati, A. Srivastava, P. Vuong, V. Ottapilakkal, Y.N. Sama, T.H. Ngo, T. Moudakir, G. Patriarche, S. Gautier, P.L. Voss, S. Sundaram, J.P. Salvestrini, and A. Ougazzaden, "Multiple Shapes Micro-LEDs with Defect Free Sidewalls and Simple Liftoff and Transfer Using Selective Area Growth on Hexagonal Boron Nitride Template," Adv Materials Technologies **8**(15), 2300147 (2023).
[35] R. Gujrati, S. Karrakchou, L. Oliverio, S. Sundaram, P.L. Voss, E. Monroy, J.P. Salvestrini, and A. Ougazzaden, "Design and fabrication process flow for high-efficiency and flexible InGaN solar cells," Micro and Nanostructures **176**, 207538 (2023).

[36] X. Li, M.B. Jordan, T. Ayari, S. Sundaram, Y. El Gmili, S. Alam, M. Alam, G. Patriarche, P.L. Voss, J. Paul Salvestrini, and A. Ougazzaden, "Flexible metal-semiconductor-metal device prototype on wafer-scale thick boron nitride layers grown by MOVPE," Sci Rep **7**(1), 786 (2017).
[37] R.D. Blevins, and R. Plunkett, "Formulas for Natural Frequency and Mode Shape," Journal of Applied Mechanics **47**(2), 461–462 (1980).
[38] N. DeRoller, M. Qazi, J. Liu, and G. Koley, "Characterization of an AlGaN/GaN Electrostatically Actuated Cantilever using Finite Element Method," (2010).
[39] M.A. Moram, Z.H. Barber, and C.J. Humphreys, "Accurate experimental determination of the Poisson's ratio of GaN using high-resolution x-ray diffraction," Journal of Applied Physics **102**(2), 023505 (2007).
[40] A. Falin, Q. Cai, E.J.G. Santos, D. Scullion, D. Qian, R. Zhang, Z. Yang, S. Huang, K. Watanabe, T. Taniguchi, M.R. Barnett, Y. Chen, R.S. Ruoff, and L.H. Li, "Mechanical properties of atomically thin boron nitride and the role of interlayer interactions," Nat Commun **8**(1), 15815 (2017).
[41] A. Ben Amar, M. Faucher, V. Brandli, Y. Cordier, and D. Théron, "Young's modulus extraction of epitaxial heterostructure AlGaN/GaN for MEMS application: Young's modulus extraction of epitaxial heterostructure AlGaN/GaN," Phys. Status Solidi A **211**(7), 1655–1659 (2014).
[42] S.J. Cartamil-Bueno, M. Cavalieri, R. Wang, S. Houri, S. Hofmann, and H.S.J. Van Der Zant, "Mechanical characterization and cleaning of CVD single-layer h-BN resonators," Npj 2D Mater Appl **1**(1), 16 (2017).
[43] X.-Q. Zheng, J. Lee, and P.X.-L. Feng, "Hexagonal boron nitride nanomechanical resonators with spatially visualized motion," Microsyst Nanoeng **3**(1), 17038 (2017).
[44] V.A.S. Kandadai, V. Gadhamshetty, and B.K. Jasthi, "Effect of buffer layer and substrate growth temperature on the microstructural evolution of hexagonal boron nitride thin films," Surface and Coatings Technology **447**, 128805 (2022).
[45] L. Nicu, P. Temple-Boyer, C. Bergaud, E. Scheid, and A. Martinez, "Energy study of buckled micromachined beams for thin-film stress measurements applied to SiO_2," J. Micromech. Microeng. **9**(4), 414–421 (1999).